Disproportionation Channel of Self-Reaction of Hydroxyl Radical, OH plus OH -> H2O + O, Studied by Time-Resolved Oxygen Atom Trapping

ARTICLE *in* THE JOURNAL OF PHYSICAL CHEMISTRY A · NOVEMBER 2012

Impact Factor: 2.69 · DOI: 10.1021/jp308885j · Source: PubMed

2 AUTHORS:

Manuvesh Sangwan
Carnegie Institution for Science
15 PUBLICATIONS **46** CITATIONS

SEE PROFILE

Lev N Krasnoperov
New Jersey Institute of Technology
161 PUBLICATIONS **1,303** CITATIONS

SEE PROFILE

THE JOURNAL OF PHYSICAL CHEMISTRY A

Article

pubs.acs.org/JPCA

Disproportionation Channel of Self-Reaction of Hydroxyl Radical, OH + OH → H_2O + O, Studied by Time-Resolved Oxygen Atom Trapping

Manuvesh Sangwan and Lev N. Krasnoperov*

Department of Chemistry and Environmental Science, New Jersey Institute of Technology University Heights, Newark, New Jersey 07102, United States

ABSTRACT: The disproportionation channel of the self-reaction of hydroxyl radicals, OH + OH → H_2O + O (1a) was studied using pulsed laser photolysis coupled to transient UV−vis absorption spectroscopy over the 298−414 K temperature and 3−10 bar pressure ranges (bath gas He). To distinguish channel 1a from the recombination channel 1b, OH + OH → H_2O_2 (1b), time-resolved trapping of oxygen atoms, produced in channel 1a, was used. The ozone produced in the reaction of oxygen atoms with molecular oxygen was measured using strong UV absorption at 253.7 nm. The results of this study (k_{1a} = (1.38 ± 0.20) × 10^{-12} $(T/300)^{-0.76}$ confirm the IUPAC recommended value of Bedjanian et al. (*J. Phys. Chem. A* **1999**, *103*, 7017−7025), as well as the negative temperature dependence over the temperature range studied, and do not confirm the ca. 1.8 higher value obtained in the most recent study of Bahng et al. (*J. Phys. Chem. A* **2007**, *111*, 3850−3861). The V-shaped temperature dependence of k_{1a} based on combined current and previous studies in the temperature range of 233−2380 K is k_{1a} = (5.1 exp(−*T*/190 K) + 0.30(*T*/300 K)$^{1.73}$) × 10^{-12} cm^3 $molecule^{-1}$ s^{-1}.

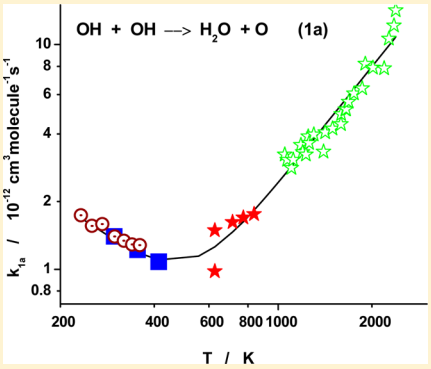

INTRODUCTION

Hydroxyl radical plays an important role both in atmospheric[3−9] and in combustion[10−16] chemistry. Self-reaction of hydroxyl radical is very important in the laboratory kinetic studies as well as for fundamental chemical kinetics:

$$OH + OH \rightarrow H_2O + O \quad (1a)$$

$$OH + OH \rightarrow H_2O_2 \quad (1b)$$

In the reaction mechanisms used in the laboratory studies of radical−radical reactions with the participation of hydroxyl radical, reaction 1 not only serves as an additional sink for hydroxyl radicals but also initiates a sequence of secondary, highly undesirable reactions of oxygen and hydrogen atoms, formed in channel 1a, and their subsequent reactions. Therefore, accurate values of the rate constant of reaction 1 as well as the branching ratios for the disproportionation channel 1a and recombination channel 1b are important. Kinetic behavior of reaction 1 is complicated due to the existence of the two channels 1a and 1b. The disproportionation channel 1a is assumed to be pressure independent; however, the recombination channel is pressure dependent over the wide range of temperatures and pressures. In addition, our recent study revealed a peculiar V-shaped temperature dependence of the rate constant of channel 1a, with negative temperature dependence at ambient and slightly elevated temperatures and positive at temperatures higher than ca. 450 K.[17]

Reaction 1 was exhaustively studied both experimentally[1,2,17−36] and theoretically.[37−46] Detailed summary of the previous works is given in recent publications.[2,17] The temperature dependence of channel 1a near ambient temperature was a subject of minor controversy in the past. A positive temperature dependence was measured in one experimental study,[17] although subsequent studies resulted in a small negative temperature dependence.[30] It appears that the negative temperature dependence of the disproportionation channel 1a is well established.

The absolute value of the rate constant of the disproportionation channel 1a is a subject of current controversy. Bedjanian et al., using discharge flow combined with mass-spectrometric detection, obtained a slightly negative temperature dependence in the range 233 to 360 K at 1 Torr of He.[1] The measured apparent activation energy was −1.7 kJ mol^{-1}, and the room temperature rate constant was 1.43 × 10^{-12} cm^3 $molecule^{-1}$ s^{-1}. Both the room temperature value of (1.4 ± 0.2) × 10^{-12} cm^3 $molecule^{-1}$ s^{-1} and the negative temperature dependence of Bedjanian et al. are currently accepted in the IUPAC recommendations.[47] However, the most recent direct measurements of Bahng and Macdonald[2] using laser pulsed photolysis coupled to time-resolved IR absorption are in significant, almost a factor of 2, disagreement with this value (2.7 ± 0.9) × 10^{-12} cm^3 $molecule^{-1}$ s^{-1}).

The purpose of this study was to resolve this discrepancy using a completely different approach. Typically, separation of the pressure independent channel from the pressure dependent recombination channel is performed via kinetic measurements at low pressures (Torr range) where the recombination channel can be neglected. This leads to difficulties caused by high wall activity toward heterogeneous reactions of a hydroxyl radical as well as potential participation of excited species. The approach used in

Received: September 6, 2012
Revised: November 2, 2012

   dx.doi.org/10.1021/jp308885j | *J. Phys. Chem. A* XXXX, XXX, XXX−XXX

this work is based on the selective measurements of channel 1a (presumably pressure independent) at elevated pressures, which allows circumventing these experimental difficulties.

The approach adopted in this study is based on the different products formed in channels 1a and 1b. Specifically, channel 1a produces oxygen atoms, which can be efficiently converted to ozone. Ozone, in turn, can be sensitively detected and quantified via the very strong and accurately characterized absorption in the UV. Provided that the trapping reaction ensures efficient conversion of oxygen atoms to ozone molecules and that the absolute concentration of hydroxyl radical is known, the approach provides reliable discrimination of the two channels in reaction 1 and independent determination of the rate constant of the disproportionation channel 1a. To make the reaction of oxygen atoms with molecular oxygen (reaction 2) sufficiently fast to ensure efficient trapping of oxygen atoms, elevated pressures of the bath gas (3−10 bar) are required.

$$O + O_2 \rightarrow O_3 \quad (2)$$

This also eliminates problems associated with the high wall reactivity of hydroxyl radicals because of the very small contribution of the diffusion limited rate constant of wall reaction at such pressures.

EXPERIMENTAL SECTION

The experimental approach is based on excimer laser photolysis coupled to UV−vis transient absorption spectroscopy and a high-pressure flow system. The details of the experimental setup and the design of the flow reactor are given in our previous works.[17,48−50] Hydroxyl radicals were generated in pulsed photolysis of N_2O in the presence of water at 193.3 nm (ArF excimer laser):

$$N_2O + h\nu(193\ nm) \rightarrow O(^1D) + N_2 \quad (P1a)$$

$$N_2O + h\nu(193\ nm) \rightarrow N(^4S) + NO(^2\Pi) \quad (P1b)$$

$$O(^1D) + H_2O \rightarrow 2OH(v = 0, 1) \quad (3a)$$

$$O(^1D) + H_2O \rightarrow O(^3P) + H_2O \quad (3b)$$

$$O(^1D) + H_2O \rightarrow H_2 + O_2 \quad (3c)$$

The quantum yield of the major channel P1a is unity within 1%; the minor channel P1b is less than 0.8%.[51]

The fraction of vibrationally excited hydroxyl radicals OH($v = 1$) formed in the reaction of $O(^1D) + H_2O$ (reaction 4a) is 22−24%.[52−54]

A fraction of $O(^1D)$ formed in photolysis of N_2O reacts with N_2O:

$$O(^1D) + N_2O \rightarrow NO + NO \quad (4a)$$

$$O(^1D) + N_2O \rightarrow O_2 + N_2 \quad (4b)$$

$$O(^1D) + N_2O \rightarrow O(^3P) + N_2O \quad (4c)$$

The kinetics of hydroxyl radical decay was monitored by absorption in the UV (multiline at ca. 308 nm using a low pressure Ar/H_2O DC discharge lamp.[17]

Before entering the reactor, the laser beam was formed (to provide uniformity) with spherical ($f = 30$ cm; the distance from the reactor, 70 cm) and cylindrical ($f = 30$ cm; the distance from the reactor, 23 cm) lenses. The beam uniformity across the reactor cross-section was ±7.3% from the mean value.

Helium was used as the bath gas in all measurements. The measurements were performed over the 25−141 °C temperature range at 3 and 10 bar. The 4-window configuration in the reactor to precisely define the path length of the reaction zone was employed.[17] The gas flow rates were controlled by high pressure mass flow controllers (Brooks, model 5850). The total flow rates of the reactant mixtures with helium were in the range 20−75 sccs. Additional flush flows to the cold reactor windows were in the range 4.5−10 sccs. Liquid H_2O was injected into the high pressure system using a precision syringe pump (Harvard Apparatus, Model PHD 4400). The flow of liquid H_2O in the range 6−18 μL/min was flowing from the syringe pump through a capillary tube to an evaporator kept at 90 °C.

The concentrations of the precursors used were $(4.6−6.4) \times 10^{16}$ molecules cm^{-3} (N_2O), $(3.7−11.0) \times 10^{17}$ (H_2O), and $(3.9−5.5) \times 10^{17}$ (O_2). The photolysis laser photon fluence inside the reactor was varied in the range $(4.6−8.9) \times 10^{15}$ photons cm^{-2} $pulse^{-1}$. The initial concentrations of hydroxyl radicals were in the range $(4.7−8.4) \times 10^{13}$ molecules cm^{-3}. The pressure range of the current study was 3−10 bar (He). The temperature range was 295−414 K. The upper temperature of the study was limited by the thermal stability of ozone. The repetition rate of the laser was adequate to ensure complete replacement of the gas mixture in the reactor between the pulses (0.3−2 Hz depending on pressure).

Reagents. Helium used in the experiments was BIPHelium from Airgas with 99.9999% purity with reduced oxygen content (<10 ppb). UHP oxygen was obtained from Matheson TriGas (99.98% purity). A certified mixture of N_2O in He (2.50%, accuracy, ±2%) obtained from Matheson Tri-Gas was used. Purified water (Milli-Q, with TOC less than 5 ppb) was degassed by freeze−pump−thaw cycles and used as a reactant supplied by a syringe pump (Harvard Apparatus PHD 4400) as well as in the low pressure H_2O/Ar discharge hydroxyl monitoring lamp. UHP Argon obtained from Matheson TriGas (99.999% purity) was used in the H_2O/Ar lamp.

RESULTS AND DISCUSSION

Transient absorption profiles of OH and O_3 were measured at 23 combinations of temperature and pressure. Sample absorption temporal profiles at 308 and 253.7 nm are shown in Figure 1. The reaction mechanism and the kinetic parameters used in the fits of

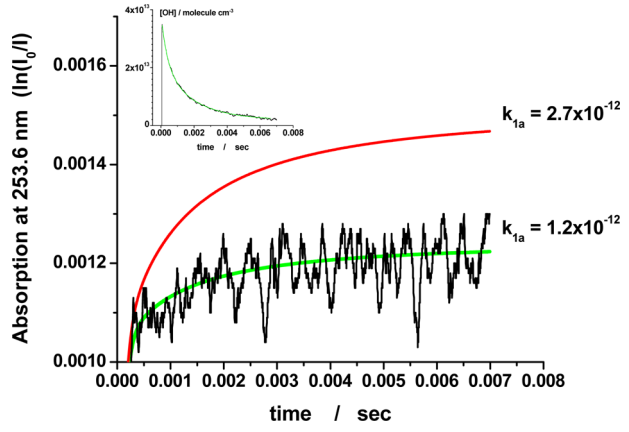

Figure 1. Sample ozone and OH (inset) absorption profiles (2.91 bar; 295 K; $[N_2O] = 5 \times 10^{16}$, $[O_2] = 4.13 \times 10^{17}$, $[OH] = 4.12 \times 10^{13}$, and $[H_2O] = 3.73 \times 10^{17}$ molecules cm^{-3}). Green line is the fit by the reaction mechanism yielding $k_{1a} = 1.2 \times 10^{-12}$ cm^3 $molecule^{-1}$ s^{-1}. Red line is the simulation using $k_{1a} = 2.7 \times 10^{-12}$ cm^3 $molecule^{-1}$ s^{-1} (ref 2). The original curve taken with the time resolution of 3 usec and 2 usec/point was smoothed by a 50 points-adjacent averaging.

dx.doi.org/10.1021/jp308885j | J. Phys. Chem. A XXXX, XXX, XXX−XXX

Table 1. Reaction Mechanism Used for Fitting the Experimental Absorption Profiles

reaction	reactants	products	rate constant[a]	ref	comments
1a	OH + OH	O + H_2O	this work		
1b		H_2O_2	k_{1b} = [He] 9.0 × $10^{-31}(T/300)^{-3.5}$	17	
			k_{inf1b} = 2.4 × 10^{-11} $(T/300)^{-0.5}$		
			F_{cent1b} = 0.37		
2	O + O_2	O_3	[M] 3.4 × $10^{-34}(T/300)^{-1.2}$	58	
3a	$O(^1D)$ + H_2O	OH + OH	1.7 × 10^{-10}exp(36/T)	59	
3b		$O(^3P)$ + H_2O	<0.003 k_{3a}	60	neglected
3c		H_2 + O_2	2.2 × 10^{-12}	61	
4a	$O(^1D)$ + N_2O	NO + NO	8.37 × 10^{-11}	branching ratio of 0.62 based on ref 61	the total rate constant (k_4 = 1.35 × 10^{-10}) is the average of three studies,[62−64] as discussed in ref 2
4b		O_2 + N_2	5.13 × 10^{-11}	branching ratio of 0.38 based on ref 61	
4c		$O(^3P)$ + N_2O	1.3 × 10^{-12}	59	k_{4c}/k_4 < 0.01,[59] set to 1.3 × 10^{-12}
5a	OH + O	O_2 + H	2.4 × 10^{-11} exp(110/T)	61	
5b		HO_2	[M] 1.6 × 10^{-31} $(T/298)^{-2.6}$	65	
6a	H + O_2	OH + O	1.62 × 10^{-10} exp (−62110/8.31447/T)	66	
6b		HO_2	1.8 × $10^{-32}(T/298)$	67	
7	HO_2 + O_2	OH + O_3	0		endothermic, neglected
8	OH + O_3	HO_2 + O_2	1.7 × 10^{-12} exp(−7820/8.31447 /T)	61	
9	O + O_3	O_2 + O_2	8.0 × 10^{-12} exp(−17130/8.31447 /T)	61	
10	H + O_3	OH + O_2	1.4 × 10^{-10} exp(3990/8.31447 /T)	63	
11	HO_2 + O_3	OH + O_2 + O_2	1.97 × 10^{-16} × $(T/298)^{4.57}$ exp (5760/8.31447/T)	61	
12a	OH + H	H_2 + O	6.86 × $10^{-14}(T/298)^{2.8}$ exp(−1950/T)	68	
12b		H_2O	[M] 1.6 × $10^{-31}(T/298)^{-2.6}$	65	
13	OH + NO	HONO	$k_{13,0}$ = 6.0 × $10^{-31}(T/300)^{-2.5}$	32	$F_{13,cent}$: fit of the data from ref 32
			$k_{13,inf}$ = 3.3 × $10^{-11}(T/300)^{-0.3}$		
			$F_{13,cent}$= 0.60 exp(91/T)		
14	OH + HO_2	H_2O + O_2	4.8 × 10^{-11} exp(250/T)	69	
15	HO_2 + NO	OH + NO_2	4.0 × 10^{-12} exp(223/T)	55	
16	OH + H_2O_2	H_2O + HO_2	2.9 × 10^{-12} exp(−109/T)	70	
17	O + HO_2	O_2 + OH	2.70 × 10^{-11} exp(224/T)	61	
18	O + H_2O_2	OH + HO_2	1.40 × 10^{-12} exp(−2000/T)	61	
19a	H + HO_2	H_2 + O_2	7.11 × 10^{-11} exp(−710/T)	71	
19b		2 OH	2.81 × 10^{-10} exp(−440/T)	71	
19c		H_2O + O	5 × 10^{-11} exp(−866/T)	71	
19d		$O(^1D)$ + H_2O	3.29 × 10^{-12}(T/298)$^{1.55}$ exp(81/ T)	51	

[a]Rate constant and concentration units, cm^3 $molecule^{-1}$ s^{-1}.

the experimental profiles are listed in Table 1. The decay of hydroxyl radicals is almost entirely controlled by reaction 1 and subsequent reaction of oxygen atoms with hydroxyl radicals. Several other reactions also contribute to the decay rate. The model performance as well as the impact of the uncertainties of the rate constants on the OH simulated profiles was discussed in detail in refs 17 and 36. The hydroxyl profiles obtained in this study were modeled based on the kinetic mechanism listed in Table 1. The OH concentration profiles are reproduced by the mechanism with the accuracy of ±5% (compared to the profiles obtained based on the absorbance traces and the apparent absorption cross-section of hydroxyl radical from ref 36).

At elevated pressures, reaction 2 is sufficiently fast to compete with the reaction of oxygen atoms with OH radicals and to provide efficient trapping of oxygen atoms. Typical trapping efficiencies in these experiments were in the range 0.79−0.92. The experimental absorption profiles of OH were converted into the hydroxyl concentration profiles based on the measured absorption cross-sections.[17] Then, the hydroxyl concentration profiles were fitted using a smooth function with sufficient number of parameters to provide adequate fitting flexibility. These profiles were then explicitly used in the fits of the ozone absorption profiles using the SCIENTIST software,[55] where unknown rate constant k_{1a} was used as a fitting parameter. The results are listed in Table 2 and shown in Figure 2. Sample simulated ozone absorption profile with the rate constant k_{1a} set as 2.7 × 10^{-12} (ref 2) is shown in Figure 1. It is apparent that the ozone yield cannot be reproduced with the rate constant of Bahng and Macdonald;[2] however, the results of current measurements are in perfect agreement with the study of Bedjanian et al.[1] The highest temperature of the current study was limited

dx.doi.org/10.1021/jp308885j | J. Phys. Chem. A XXXX, XXX, XXX−XXX

Table 2. Experimental Conditions and the Rate Constant for Reaction 1a

p (bar)	T (K)	number density[a]/10^{20}	$[N_2O]_0$/10^{16}	$[H_2O]_0$/10^{17}	$[O_2]_0$/10^{17}	[NO]/10^{12}[b]	[H]/10^{12}	photon fluence/10^{15}	[OH]/10^{13}	[O]/10^{12}	$k_{1a}/10^{-12}$ cm^3 molecule^{-1} s^{-1}	$k_{1a}/10^{-12}$ cm^3 molecule^{-1} s^{-1}[c]
2.91	295	0.713	5.0	3.73	4.13	2.91	4.04	7.17	4.83	6.85	1.71	1.40 ± 0.17
2.91	295	0.713	5.0	3.73	4.13	2.87	3.99	7.08	4.77	6.76	1.52	
2.91	295	0.713	5.0	3.73	4.13	2.88	3.95	7.01	4.73	6.69	1.20	
9.88	296	2.40	6.39	4.44	5.47	4.36	5.33	7.95	6.69	1.05	1.36	
9.88	295	2.41	6.41	4.45	5.49	4.55	5.38	8.0	6.97	1.09	1.07	
9.88	295	2.41	6.41	4.45	5.49	4.48	5.29	7.86	6.85	1.07	1.36	
9.88	295	2.41	6.41	4.45	5.49	4.37	5.17	7.68	6.69	1.05	1.60	
9.88	354	1.99	5.28	11.0	4.52	1.69	1.26	7.86	8.43	4.68	1.37	1.22 ± 0.14
9.88	354	1.99	5.28	11.0	4.52	1.66	1.24	7.45	8.30	4.60	1.57	
9.88	354	1.99	5.30	3.68	4.54	4.69	4.71	8.61	7.10	10.7	1.12	
9.88	354	1.99	5.30	3.68	4.54	4.50	4.68	8.42	6.81	10.5	1.14	
9.88	354	1.99	5.30	3.68	4.54	4.59	4.68	6.61	5.46	8.48	1.09	
9.88	354	1.99	5.30	3.68	4.54	4.69	4.71	6.62	5.46	8.49	1.06	
9.88	354	1.99	5.30	3.68	4.54	4.50	4.68	6.55	5.40	8.40	1.17	
9.88	414	1.72	4.55	9.49	3.90	1.48	9.35	6.52	7.12	3.89	1.09	1.08 ± 0.07
9.88	414	1.72	4.55	9.49	3.90	1.46	9.47	6.61	7.21	3.94	1.09	
9.88	414	1.72	4.55	9.49	3.90	1.46	9.36	6.53	7.12	3.89	1.05	
9.88	414	1.72	4.55	9.49	3.90	1.46	9.35	6.50	7.11	3.89	1.08	
9.88	414	1.72	4.55	9.49	3.90	1.46	9.36	6.53	7.12	3.89	1.05	
9.88	414	1.72	4.57	3.17	3.91	4.02	3.54	7.38	6.03	9.30	1.16	
9.88	414	1.72	4.57	3.17	3.91	3.77	3.32	6.92	5.66	8.73	1.17	
9.88	414	1.72	4.57	3.17	3.91	3.72	3.28	6.84	5.59	8.62	1.13	
9.88	414	1.72	4.55	9.49	3.90	1.08	6.94	4.84	5.28	2.88	0.858	

[a]All concentrations in molecules cm^{-3}. [b]The concentrations of NO, H, and O listed are the initial concentrations after completion of all processes associated with O(^{1}D), which occur on the nanosecond time scale (<30 ns). [c]The average value of k_{1a} measured at the same conditions; the error indicated is ±2 SD of the average values (±2 SE).

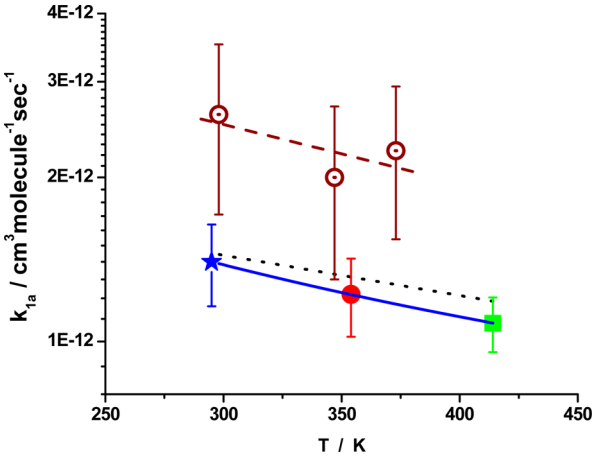

Figure 2. Rate constant of the disproportionation channel 1a compared to other experimental studies. Empty circles: Bahng and Macdonald.[2] Dotted line: Bedjanian et al.[1] Filled star, 3 and 10 bar; 295 K; filled circle, 10 bar, 354 K; filled square, 10 bar, 414 K; solid line, fit by the power dependence (see text) (this work). Each point is an average of several experiments from Table 2. The error bars combine the statistical error and the error of the absorption cross-section of OH radical (±2 SD of the average values + 0.05 k_{1a}).

by the equilibrium constant of the ozone formation reaction. At temperatures above ca. 450 K dissociation of ozone becomes important, and O-atoms cannot be efficiently converted to ozone. The temperature dependence of the absorption cross-section of ozone at 253.7 nm was taken from ref 56. Utilizing the explicit OH concentration profiles allows drastic reduction of the sensitivity of the results to the model parameters. For example, turning off reaction 1b (setting its rate constant to zero) has only 5% impact on the returned rate constant of reaction 1a. The sensitivity of the k_{1a} returned by the fits to the variation of the rate constants in the mechanism listed in Table 1 was assessed. Exclusion of all reactions except for 1a, 2 and 5a has only 1.1% impact on the returned rate constant k_{1a}. All reactions except 1b, 5a, 5b, 6a, 6b, 13, 14, and 16 have absolutely negligible impact on the returned k_{1a} (less than 0.1%). Separately turning off reactions 1b, 5b, 6a, 13, 14, and 16 lead to +5, −2, +5, +2, −5, and 0.5%, change of k_{1a}, respectively. Variation of the rate constant of reaction 6b 10 times has no impact on the rate constant k_{1a} provided that the reaction 6b is present in the mechanism. Variation of the rate constant of reaction 2 (O + O_2) by 12% leads to 0.07% change in k_{1a}. Finally, variation of the rate constants of reaction 5a (O + OH) by 23% leads to the change in k_{1a} of 0.4%. Such remarkable stability of the determined rate constant k_{1a} toward the model parameters variation is due entirely to the usage of explicit concentration profiles of OH, which are determined with the accuracy of the OH absorption cross-section (±5%). Combining all uncertainties (the uncertainty of OH concentrations, uncertainty introduced by the model, and the uncertainty associated with the noise in ozone absorption profiles), the 1σ uncertainty of k_{1a} is estimated as ca. 10−12%. This is reasonably consistent with the scatter of the measurements at the same conditions (Table 1), where the standard deviation at 298 K is estimated as ±16% from seven measurements at ambient temperature.

The results of this study, combined with the results of Bedjanian et al.,[1] the results of our previous measurements at elevated temperatures,[17] and the latest shock tube measurements of Wooldridge et al.[34] are shown in Figure 3. The results confirm the existence of the turning point in the temperature dependence of k_{1a} in the range 400−550 K.[17] The V-shaped temperature

dx.doi.org/10.1021/jp308885j | J. Phys. Chem. A XXXX, XXX, XXX−XXX

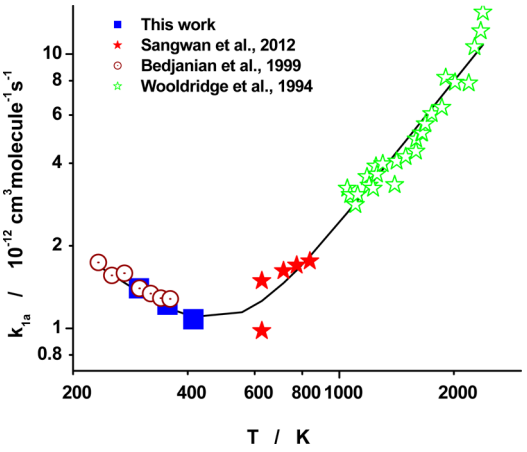

Figure 3. Rate constant of channel 1a (OH + OH → H_2O + O). Filled square, this work; dotted circles, Bedjanian et al.;[1] filled stars, Sangwan et al.;[17] empty stars, Wooldridge et al.;[34] solid line, eq E1.

dependence of k_{1a} based on combined current and previous studies in the temperature range of 233−2380 K is

$$k_{1a} = (5.1\exp(-T/190\text{ K}) + 0.30(T/300\text{ K})^{1.73}) \times 10^{-12}\text{ cm}^3\text{ molecule}^{-1}\text{ s}^{-1} \quad \text{(E1)}$$

In fact, pressure independence of the disproportionation channel 1a is an assumption that is typically made for simple metathesis reactions. V-shaped temperature dependences are likely for reactions with so-called negative barriers, when the ground state of the transition state (the bottleneck position on the PES) lies below the ground state of the reactants. For such reactions, pressure dependence of the rate constant might be anticipated (Krasnoperov et al.[57]). However, noticeable pressure dependence is expected at low temperatures and high pressures (>100 bar). In this study, no impact of pressure was found within the experimental scatter between 3 and 10 bar of the bath gas pressure. It should be noted, that theoretical calculations result in small positive barriers (0 to 1.6 kcal mol^{-1}; refs 38, 42, and 46) for reaction 1a; however, the accuracy is not sufficient to make a definite conclusion.

CONCLUSIONS

The rate constant of reaction 1a was measured over the temperature range 295−414 K at 3 and 10 bar. The disproportionation (presumably pressure independent) channel of reaction 1, OH + OH → H_2O + O, was isolated using conversion of oxygen atoms, produced in the reaction, to ozone. The rate constants were determined based on the time-resolved ozone yield using explicit OH concentration profiles. The results are consistent with the measurements of Bedjanian et al.[1] (which is currently recommended by IUPAC) and do not support the most recent measurement of Bahng and Macdonald.[2] Measured in this work, the rate constant of reaction 1a at 298 K is $k_{1a} = (1.39 \pm 0.24) \times 10^{-12}$ cm^3 molecule^{-1} s^{-1}, with the temperature dependence of the rate constant of $k_{1a} = (1.38 \pm 0.24) \times 10^{-12}\ (T/300)^{-0.76}$ in the temperature range 295−440 K. A turning point in the temperature dependence of k_{1a} in the temperature range of 400−500 K is confirmed. Such behavior is anticipated for reactions with negative barriers (Krasnoperov et al.[57]).

AUTHOR INFORMATION

Corresponding Author

*Fax: (973)-596-8436. E-mail: krasnoperov@adm.njit.edu.

Notes

The authors declare no competing financial interest.

ACKNOWLEDGMENTS

This material is based upon work supported by the National Science Foundation under Grant No. CBET-0827398.

REFERENCES

(1) Bedjanian, Y.; Le Bras, G.; Poulet, G. *J. Phys. Chem. A* **1999**, *103*, 7017−7025.
(2) Bahng, M.-K.; Macdonald, R. G. *J. Phys. Chem. A* **2007**, *111*, 3850−3861.
(3) Atkinson, R. *Chem. Rev.* **1986**, *86*, 69−201.
(4) Lelieveld, J.; Dentener, F. J.; Peters, W.; Krol, M. C. *Atmos. Chem. Phys.* **2004**, *4*, 2337−2344.
(5) Finlayson-Pitts, B. J.; Pitts, J. N. *Science* **1997**, *276*, 1045−1051.
(6) Calvert, J. G.; Derwent, R. J.; Orlando, J. J.; Tyndall, J. S.; Wallington, T. J. *Mechanisms of Atmospheric Oxidation of the Alkanes*; Oxford University Press: New York, 2008.
(7) Ravishankara, A. R. *Annu. Rev. Phys. Chem.* **1988**, *39*, 367−394.
(8) Montzka, S. A.; Krol, M.; Dlugokencky, E.; Hall, B.; Jöckel, P.; Lelieveld, J. *Science* **2011**, *331*, 67−69.
(9) Smith, I. W. M.; Ravishankara, A. R. *J. Phys. Chem. A* **2002**, *106*, 4798−4807.
(10) Smith, R. H. *Coal Res. CSIRO* **1967**, *32*, 9−18.
(11) Westbrook, C. K. *Proc. Combust. Inst.* **2000**, *28*, 1563−1577.
(12) Miller, J. A.; Pilling, M. J.; Troe, J. *Proc. Combust. Inst.* **2005**, *30*, 43−88.
(13) Warnatz, J. *Combust. Sci. Technol.* **1983**, *34*, 177−200.
(14) Haber, F. *Angew. Chem.* **1929**, *42*, 745−751.
(15) Kondrat'ev, V. N. *Usp. Khim.* **1939**, *8*, 195−240.
(16) Tsang, W. *Chem. Phys. Processes Combust.* **2009**.
(17) Sangwan, M.; Chesnokov, E. N.; Krasnoperov, L. N. *J. Phys. Chem. A* **2012**, *116*, 6282−6294.
(18) Kaufman, F.; Del Greco, F. P. *Symp. Int. Combust. Proc.* **1962**, 659−666.
(19) Caldwell, J.; Back, R. A. *Trans. Faraday Soc.* **1965**, *61*, 1939−1945.
(20) Dixon-Lewis, G.; Wilson, W. E.; Westenberg, A. A. *J. Chem. Phys.* **1966**, *44*, 2877−2884.
(21) Wilson, W. E., Jr.; O'Donovan, J. T. *J. Chem. Phys.* **1967**, *47*, 5455−5457.
(22) Mulcahy, M. F. R.; Smith, R. H. *J. Chem. Phys.* **1971**, *54*, 5215−5221.
(23) McKenzie, A.; Mulcahy, M. F. R.; Steven, J. R. *J. Chem. Phys.* **1973**, *59*, 3244−3254.
(24) Westenberg, A. A.; DeHaas, N. *J. Chem. Phys.* **1973**, *58*, 4066−4071.
(25) Clyne, M. A. A.; Down, S. *J. Chem. Soc., Faraday Trans. 2* **1974**, *70*, 253−266.
(26) Farquharson, G. K.; Smith, R. H. *Aust. J. Chem.* **1980**, *33*, 1425−1435.
(27) Trainor, D. W.; Von Rosenberg, C. W., Jr. *J. Chem. Phys.* **1974**, *61*, 1010−1015.
(28) Zellner, R.; Ewig, F.; Paschke, R.; Wagner, G. *J. Phys. Chem.* **1988**, *92*, 4184−4190.
(29) Wagner, G.; Zellner, R. *Ber. Bunsenges. Phys. Chem.* **1981**, *85*, 1122−1128.
(30) Sun, H.; Li, Z. *Chem. Phys. Lett.* **2004**, *399*, 33−38.
(31) Forster, R.; Frost, M.; Fulle, D.; Hamann, H. F.; Hippler, H.; Schlepegrell, A.; Troe, J. *J. Chem. Phys.* **1995**, *103*, 2949−2958.
(32) Fulle, D.; Hamann, H. F.; Hippler, H.; Troe, J. *J. Chem. Phys.* **1998**, *108*, 5391−5397.
(33) Ernst, J.; Wagner, H. G.; Zellner, R. *Ber. Bunsenges. Phys. Chem.* **1977**, *81*, 1270−1275.
(34) Wooldridge, M. S.; Hanson, R. K.; Bowman, C. T. *Int. J. Chem. Kinet.* **1994**, *26*, 389−401.
(35) Sutherland, J. W.; Patterson, P. M.; Klemm, R. B. *Symp. Int. Combust. Proc.* **1991**, *23*, 51−57.

(36) Sangwan, M.; Chesnokov, E. N.; Krasnoperov, L. N. *J. Phys. Chem. A* **2012**, *116*, 8661−8670.
(37) Harding, L. B.; Wagner, A. F. *Symp. Int. Combust. Proc.* **1989**, *22*, 983−989.
(38) Karkach, S. P.; Osherov, V. I. *J. Chem. Phys.* **1999**, *110*, 11918−11927.
(39) Kuhn, B.; Rizzo, T. R.; Luckhaus, D.; Quack, M.; Suhm, M. A. *J. Chem. Phys.* **1999**, *111*, 2565−2587.
(40) Brouwer, L.; Cobos, C. J.; Troe, J.; Duebal, H. R.; Crim, F. F. *J. Chem. Phys.* **1987**, *86*, 6171−6182.
(41) Maergoiz, A. I.; Nikitin, E. E.; Troe, J. *J. Chem. Phys.* **1995**, *103*, 2083−2091.
(42) Braunstein, M.; Panfili, R.; Shroll, R.; Bernstein, L. *J. Chem. Phys.* **2005**, *122*, 184307.
(43) Troe, J.; Ushakov, V. G. *Phys. Chem. Chem. Phys.* **2008**, *10*, 3915−3924.
(44) Harding, L. B. *J. Phys. Chem.* **1991**, *95*, 8653−8660.
(45) Sellevag, S. R.; Georgievskii, Y.; Miller, J. A. *J. Phys. Chem. A* **2008**, *112*, 5085−5095.
(46) Deyerl, H.-J.; Clements, T. G.; Luong, A. K.; Continetti, R. E. *J. Chem. Phys.* **2001**, *115*, 6931−6940.
(47) IUPAC Subcommittee on Gas Kinetic Data Evaluation, 2001. http://www.iupac-kinetic.ch.cam.ac.uk.
(48) Grebenkin, S. Y.; Krasnoperov, L. N. *J. Phys. Chem. A* **2004**, *108*, 1953−1963.
(49) Krasnoperov, L. N.; Chesnokov, E. N.; Stark, H.; Ravishankara, A. R. *J. Phys. Chem. A* **2004**, *108*, 11526−11536.
(50) Krasnoperov, L. N.; Chesnokov, E. N.; Stark, H.; Ravishankara, A. R. *Proc. Combust. Inst.* **2005**, *30*, 935−943.
(51) Greenblatt, G. D.; Ravishankara, A. R. *J. Geophys. Res.* **1990**, *95*, 3539−3547.
(52) Butler, J. E.; Talley, L. D.; Smith, G. K.; Lin, M. C. *J. Chem. Phys.* **1981**, *74*, 4501−4508.
(53) Sauder, D. G.; Stephenson, J. C.; King, D. S.; Casassa, M. P. *J. Chem. Phys.* **1992**, *97*, 952−961.
(54) Tanaka, N.; Takayanagi, M.; Hanazaki, I. *Chem. Phys. Lett.* **1996**, *254*, 40−46.
(55) *SCIENTIST*; Micromath Scientific Software: Saint Louis, MO.
(56) Astholz, D. C.; Croce, A. E.; Troe, J. *J. Phys. Chem.* **1982**, *86*, 696−699.
(57) Krasnoperov, L. N.; Peng, J.; Marshall, P. In *16th International Symposium on Gas Kinetics*, July 23−27, 2000, Cambridge, U.K.; p PA9.
(58) Hippler, H.; Rahn, R.; Troe, J. *J. Chem. Phys.* **1990**, *93*, 6560−6569.
(59) Vranckx, S.; Peeters, J.; Carl, S. *Phys. Chem. Chem. Phys.* **2010**, *12*, 9213−9221.
(60) Carl, S. A. *Phys. Chem. Chem. Phys.* **2005**, *7*, 4051−4053.
(61) Atkinson, R.; Baulch, D. L.; Cox, R. A.; Crowley, J. N.; Hampson, R. F.; Hynes, R. G.; Jenkin, M. E.; Rossi, M. J.; Troe, J. *Atmos. Chem. Phys.* **2004**, *4*, 1461−1738.
(62) Takahashi, K.; Takeuchi, Y.; Matsumi, Y. *Chem. Phys. Lett.* **2005**, *410*, 196−200.
(63) Atkinson, R.; Baulch, D. L.; Cox, R. A.; Hampson, R. F.; Kerr, J. A.; Troe, J. *J. Phys. Chem. Ref. Data* **1989**, *18*, 881−1097.
(64) Dunlea, E. J.; Ravishankara, A. R. *Phys. Chem. Chem. Phys.* **2004**, *6*, 2152−2161.
(65) Zellner, R.; Erler, K.; Field, D. *Symp. Int. Combust. Proc.* **1977**, *16*, 939−948.
(66) Baulch, D. L.; Cobos, C. J.; Cox, R. A.; Frank, P.; Hayman, G.; Just, T.; Kerr, J. A.; Murrells, T.; Pilling, M. J.; Troe, J.; Walker, R. W.; Warnatz, J. *J. Phys. Chem. Ref. Data* **1994**, *23*, 847−1033.
(67) Michael, J. V.; Su, M. C.; Sutherland, J. W.; Carroll, J. J.; Wagner, A. F. *J. Phys. Chem. A* **2002**, *106*, 5297−5313.
(68) Tsang, W.; Hampson, R. F. *J. Phys. Chem. Ref. Data* **1986**, *15*, 1087−1279.
(69) Keyser, L. F. *J. Phys. Chem.* **1988**, *92*, 1193−1200.
(70) Atkinson, R. B., D.L; Baulch, D. L.; Cox, R. A.; Hampson, R. F., Jr.; Kerr, J. A.; Rossi, M. J.; Troe, J. *J. Phys. Chem. Ref. Data* **1997**, *26*, 1329−1499.
(71) Baulch, D. L.; Cobos, C. J.; Cox, R. A.; Esser, C.; Frank, P.; Just, T.; Kerr, J. A.; Pilling, M. J.; Troe, J.; et al. *J. Phys. Chem. Ref. Data* **1992**, *21*, 411−734.